Supporting Information

Thiophosphate Bioisosteres of Inositol Hexakisphosphate Enhances Binding Affinity and Residence Time to Bacterial Virulence Factors.

Rebecca Cummer,[1] Garvit Bhatt,[1,2] Lauren M. Finn,[3] Bettina G. Keller,[3] Bhushan Nagar,[2] and Bastien Castagner[1,*]

[1]Department of Pharmacology and Therapeutics, [2]Department of Biochemistry, McGill University, Montréal, Québec H3G 1Y6, Canada. [3]Department of Biology, Chemistry, Pharmacy, Freie Universität, Arnimallee 22, 14195 Berlin, Germany. *Email: bastien.castagner@mcgill.ca. Tel.: 514-398-2181. Fax: 514-398-2045.

Table of Contents

1. Supplementary Figures

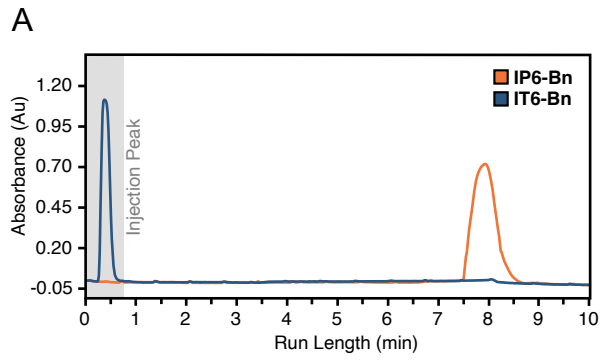

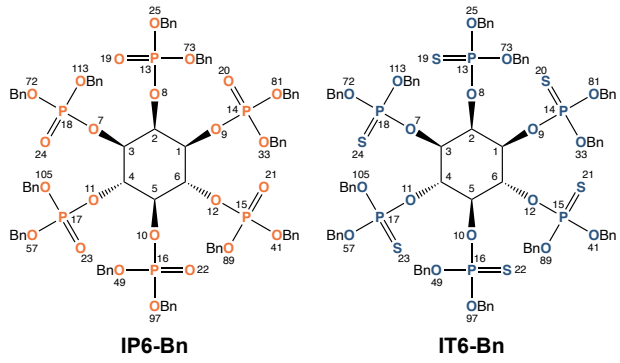

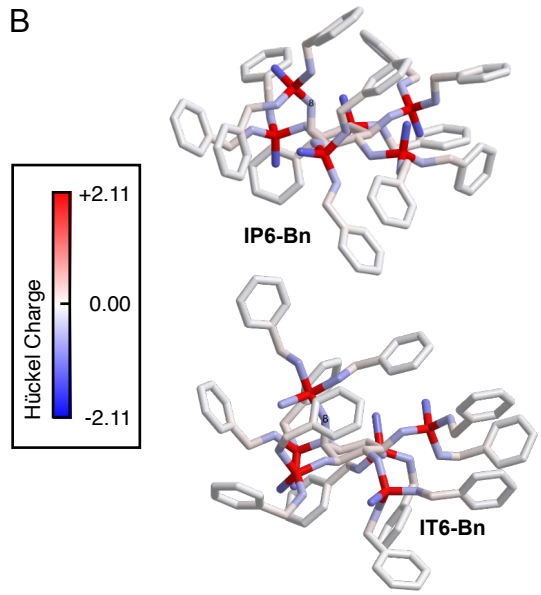

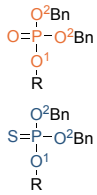

Table S1. Average Hükel Charge per element for **IP6-Bn** and **IT6-Bn**, mean ± SD.

Element	IP6-Bn	IT6-Bn	P-value Summary
O Oxo/**S** Thio	-1.16 (0.0043)	-0.86 (0.15)	*
O Ether 1	-0.49 (0.023)	-0.53 (0.047)	*
O Ether 2	-0.48 (0.029)	-0.53 (0.063)	**
P Phosphine	2.11 (0.0057)	1.97 (0.017)	*

Polar Surface Area	286.56 Å²	166.14 Å²

Figure S1. Lipophilicity differences between **IP6-Bn** and **IT6-Bn**. (A) UV chromatogram (215 nm) of **IP6-Bn** and **IT6-Bn** on a SepaFlash normal-phase column in 0–10% methanol/dichloromethane at 18 mL/min. (B) To explain the differences in cLogP we determined the Hückel charge of each element for both compounds. Structural representation of **IP6-Bn** and **IT6-Bn** in their geometry optimized/energy minimized configurations. Each element is colored in accordance with their Hückel charge. The average Hückel charge for each element type in the phosphate and thiophosphate functional groups are noted. The calculated charges for each element type were compared with a Welch's t-test (n = 6) in Prism 10 and the correspondent p-values are noted, * $p \leq 0.05$, ** $p \leq 0.01$. **IP6-Bn** phosphine and the ethers on positions 1 and 2 were more positively charged than on **IT6-Bn**, whereas the phosphoryl group was more negatively charged than the phosphorus thioate on **IP6-Bn**. Since the phosphoryl is more electronegative than the phosphorus thioate it has a greater inductive effect, resulting in less charge density on the ethers. As a result, the charge distribution is greater for **IP6-Bn**, which was reflected in its significantly higher polar surface area noted in Table S1 (286.56 Å^2 vs. 166.14 Å^2). (C) Atom labelling of **IP6-Bn** and **IT6-Bn**, as used in Table S1.

Table S2. Raw dataset for the Hückel charge calculations. P-value was determined by comparing the charge difference for each atom type to zero with a Wilcoxon Test.

Atom	Atom Type (MM2)	IP6-Bn Charge (Hückel)	IT6-Bn Charge (Hückel)	Charge Difference
O(7)	O Ether	-0.5022	-0.5128	-0.01064
O(8)	O Ether	-0.4519	-0.6295	-0.1776
O(9)	O Ether	-0.4928	-0.5084	-0.01555
O(10)	O Ether	-0.5041	-0.5189	-0.01474
O(11)	O Ether	-0.5202	-0.5247	-0.004537
O(12)	O Ether	-0.4996	-0.5146	-0.01503
			p-value	0.031
P(13)	P Phosphine	2.1087	2.0023	0.1064
P(14)	P Phosphine	2.1126	1.9636	0.1490
P(15)	P Phosphine	2.1049	1.9573	0.1475
P(16)	P Phosphine	2.1055	1.9598	0.1457
P(17)	P Phosphine	2.1105	1.9607	0.1498
P(18)	P Phosphine	2.0963	1.9569	0.1394
			p-value	0.031
O/S(19)	O oxo/S Thio	-1.1676	-0.5523	0.6153
O/S(20)	O oxo/S Thio	-1.1632	-0.9353	0.2280
O/S(21)	O oxo/S Thio	-1.1690	-0.9251	0.2439
O/S(22)	O oxo/S Thio	-1.1675	-0.9238	0.2436
O/S(23)	O oxo/S Thio	-1.1590	-0.9281	0.2309
O/S(24)	O oxo/S Thio	-1.1708	-0.9131	0.2576
			p-value	0.031
O(25)	O Ether	-0.5040	-0.6593	-0.1553
O(33)	O Ether	-0.5185	-0.4898	0.0286
O(41)	O Ether	-0.4487	-0.4991	-0.0504
O(49)	O Ether	-0.5027	-0.4882	0.0145
O(57)	O Ether	-0.4447	-0.4957	-0.0510
O(65)	O Ether	-0.4875	-0.5054	-0.01787
O(73)	O Ether	-0.4925	-0.6704	-0.1778
O(81)	O Ether	-0.4468	-0.5107	-0.06389
O(89)	O Ether	-0.5060	-0.5322	-0.02625
O(97)	O Ether	-0.4463	-0.5285	-0.08220
O(105)	O Ether	-0.5001	-0.5129	-0.01286
O(113)	O Ether	-0.4522	-0.5121	-0.05994
			p-value	0.0093

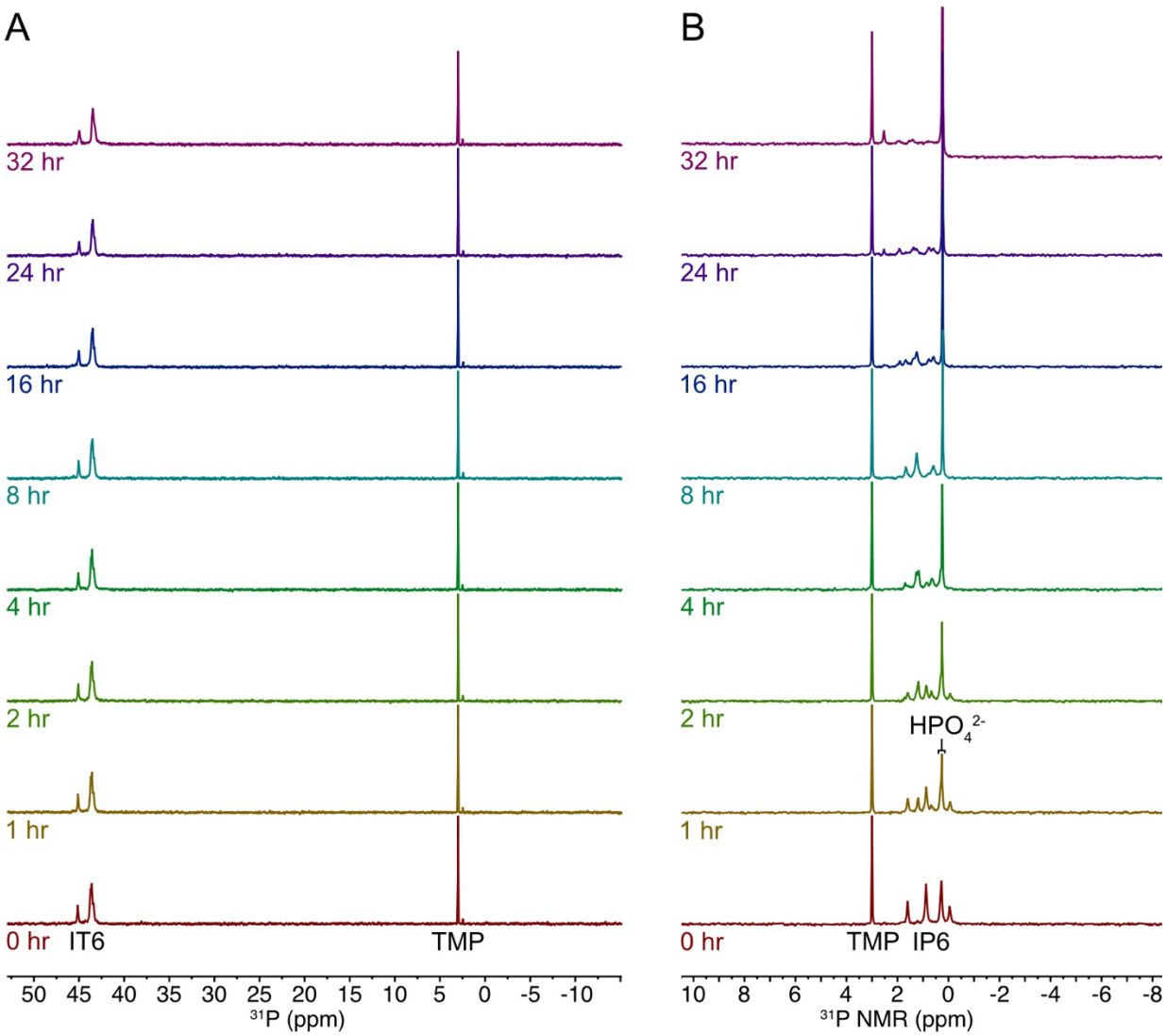

Figure S2. Stacked phosphorus NMR spectra (^{31}P with ^{1}H decoupling) of 4 mM **IT6** (A) or **IP6** (B) in the presence of phytase-4 in 100 mM acetate buffer, 10% D_2O, pH 5 over 32 h. All spectra have the internal standard 4 mM trimethyl phosphate (TMP) to track the quantity of substrate. **IP6** degradation shows the appearance of free phosphate (HPO_4^{-2}) after 1 h.

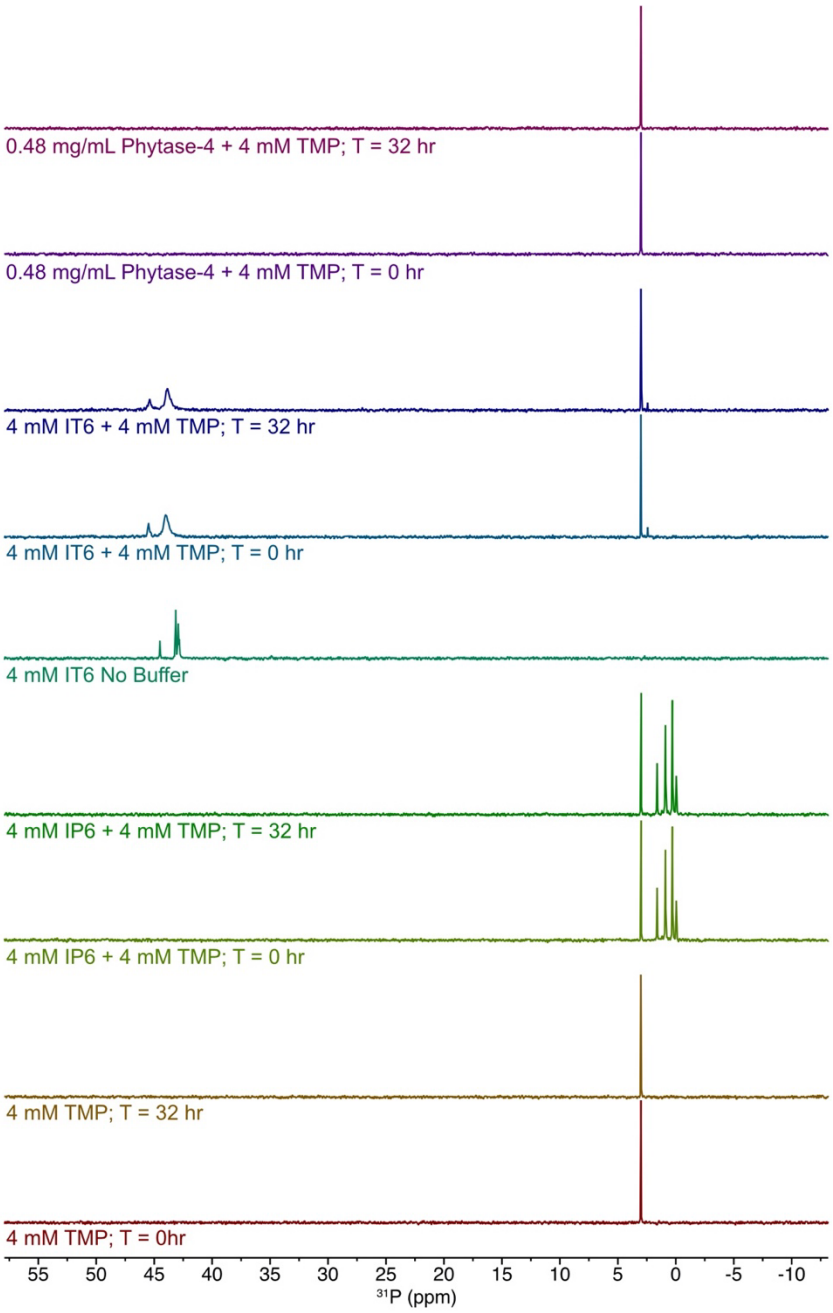

Figure S3. Stacked phosphorus NMR spectra (^{31}P with ^{1}H decoupling) of the control groups used in the phytase degradation assay. The controls (from bottom to top) consist of the internal standard alone, **IP6** alone, **IT6** alone, and phytase-4 alone. The samples with the internal standard alone contain 4 mM trimethyl phosphate (TMP), in 100 mM acetate buffer, pH 5, 10% D_2O at time 0 and 32 h. The samples with **IP6** alone contain 4 mM **IP6** and 4 mM TMP in 100 mM acetate buffer, pH 5, 10% D_2O at time 0 and 32 h. The samples with **IT6** alone contains 4 mM **IT6** in D_2O and 4 mM **IT6** and 4 mM TMP in 100 mM acetate buffer, pH 5, 10% D_2O at time 0 and 32 h. The samples with phytase-4 alone contains 0.48 mg/mL phytase-4 and 4 mM TMP in 100 mM acetate buffer, pH 5, 10% D_2O at time 0 and 32 h.

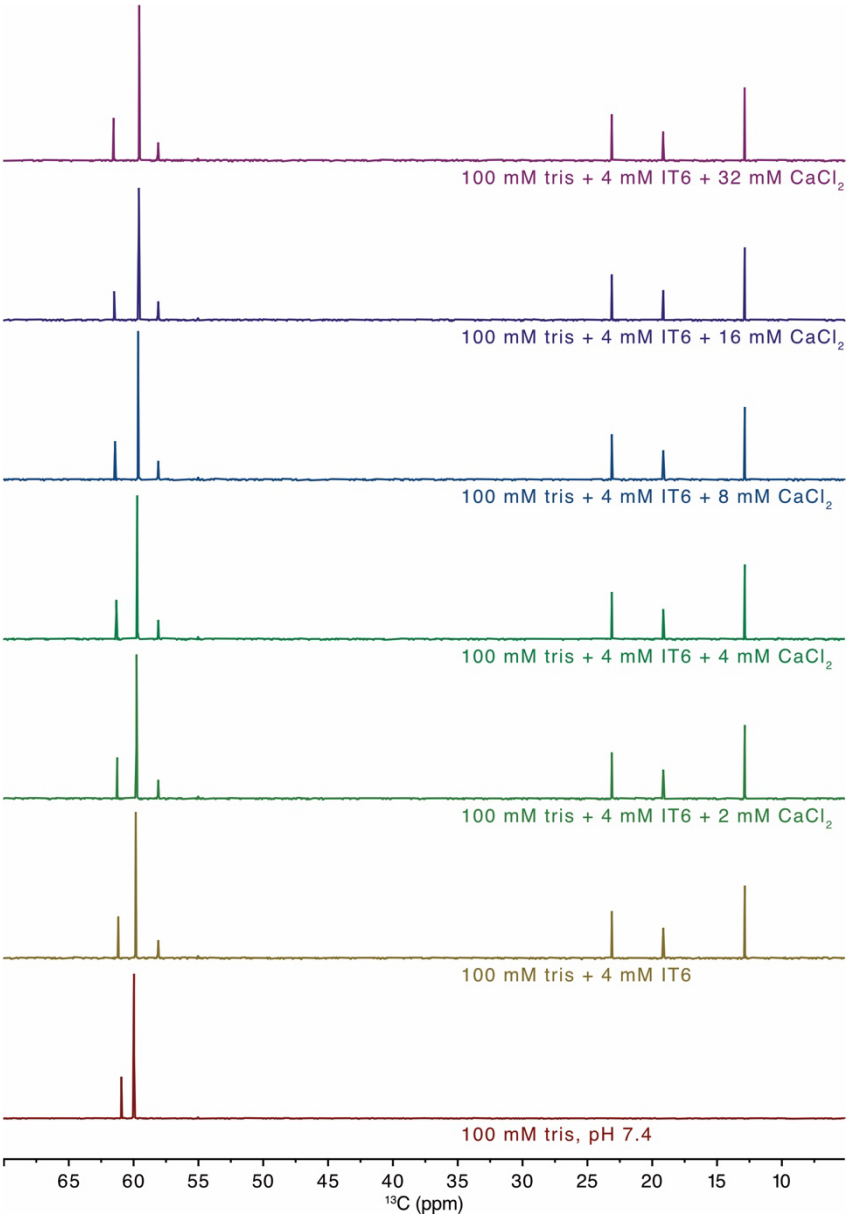

Figure S4. Stacked carbon NMR spectra (^{13}C) of **IT6** in 100 mM tris buffer, pH 7.4 with varied concentrations of $CaCl_2$. The lack of a change in the **IT6** carbon spectrum indicates that there is no ring flipping associated with the complex formation of **IT6-Ca**.

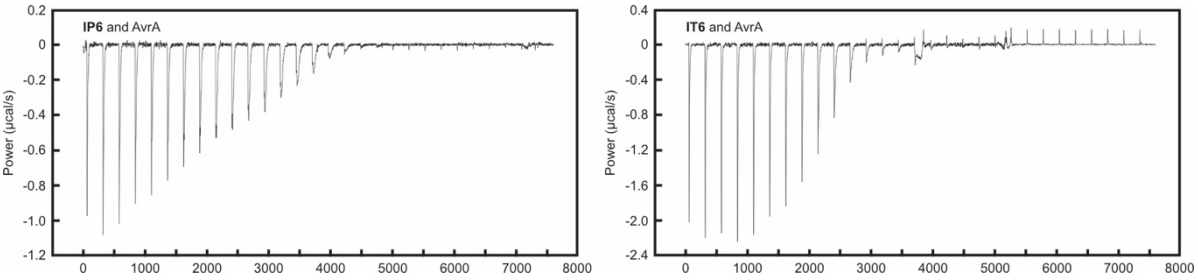

Figure S5. Raw datasets of the isothermal calorimetry (ITC) experiments performed to determine the dissociation constants (K_d) and the k_{off} of **IP6** (A) and **IT6** (B) with AvrA.

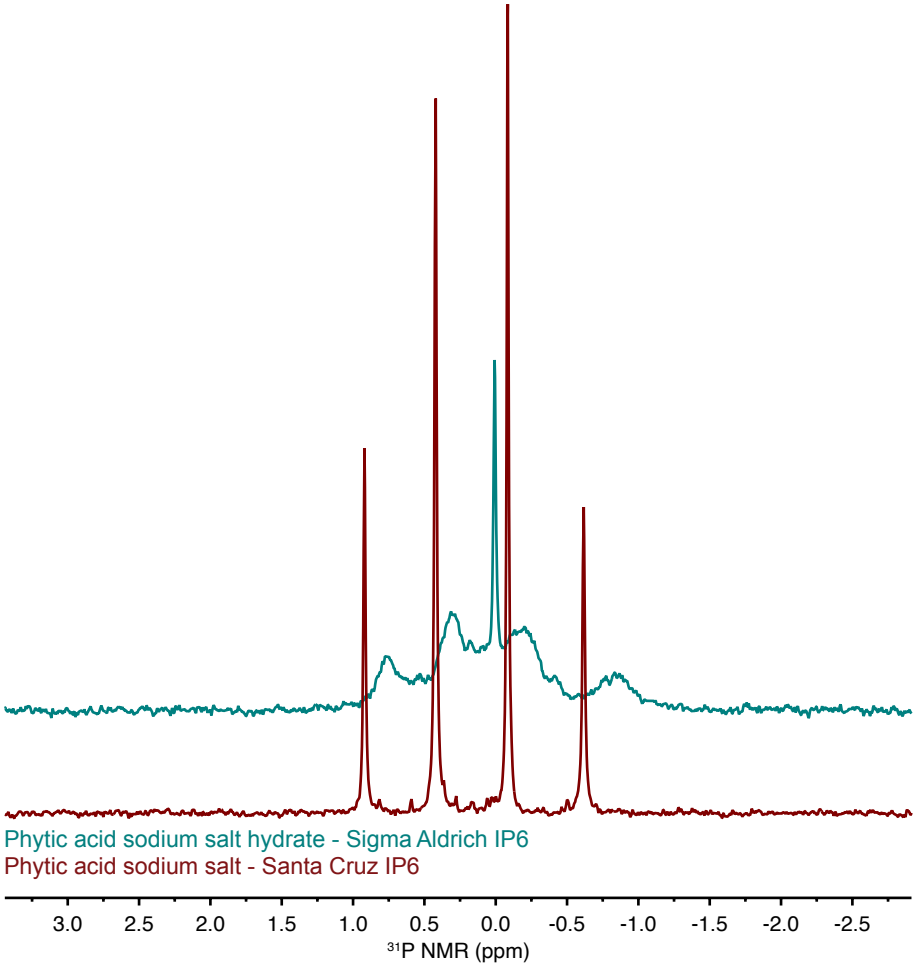

Figure S6. Overlapped ^{31}P NMR spectra of phytic acid (**IP6**) with different molecular compositions at pH 3. The red spectrum corresponds with **IP6** in its sodium salt form. The teal spectrum corresponds with **IP6** with water of crystallization which has undergone hydrolysis and shows free phosphate groups at ~0 ppm. To note: both of these compounds have been stored at room temperature for >5 years.

2. Methods and General Procedures

Reagents

Reagent or Resource	Source	Identifier
Biological Samples		
native wheat phytase (phytase-4)	Creative Enzymes	Cat# NATE-0566
Escherichia coli BL21 DE3	New England Biolabs	Cat# C2527H
ubl-specific protease (ULP) 1	Fisher Scientific	Cat# 12588018
Chemicals		
acetic anhydride	Sigma-Aldrich	Cat# 320102-1L
chloroform-d	Acros Organics N.V.	Cat# AC166251000
deuterium Oxide (D_2O)	ACP Chemicals	Cat# DLM-4-25
dichloromethane	Sigma-Aldrich	Cat# D65100-4L
dithiothreitol (DTT)	Fisher Scientific	Cat# BP17225
DNase I, grade II	Roche	Cat# 10104159001
dowex® 50W X8, p.a. H+-form, 200–400 mesh	Sigma-Aldrich	Cat# 44519-100G
glycerol	Sigma-Aldrich	Cat# G2025
HEPES sodium	Sigma-Aldrich	Cat# H7006-500G
hydrochloric acid	Fisher Scientific	Cat# A144S-500
imidazole	Fisher Scientific	Cat# 288-32-4
isopropyl β-d-1-thiogalactopyranoside (IPTG)	BioBasic Inc.	Cat# IB0168
kanamycin sulfate	Fisher Scientific	Cat# BP906
LB broth miller	BioShop Canada Inc.	Cat# LBL407
methanol	Sigma-Aldrich	CAS No. 67-56-1
phenylmethanesulfonyl fluoride (PMSF)	Sigma-Aldrich	CAS No. 329-98-6
phytic acid sodium salt	Santa Cruz Biotechnology	Cat# sc-250718A
sodium acetate trihydrate	BioShop Canada Inc.	Cat# SAA555.1
sodium chloride	Fisher Scientific	Cat# S2771-1
SYPRO orange protein gel stain	Invitrogen	Cat# S6650
trimethyl phosphate	Sigma-Aldrich	Cat# 241024-50G
tris (2-carboxyethyl) phosphine hydrochloride (TCEP)	Sigma-Aldrich	Cat# C4706-2G
Software and Algorithms		
AFFINImeter		https://www.affinimeter.com/site/software/
Affinity Designer 2	Serif Ltd.	https://affinity.serif.com/en-us/designer/
Chem3D version 22.2.0.3300	PerkinElmer Informatic, Inc.	https://revvitysignals.com/products/research/chemdraw
ChemDraw 22.2.0	PerkinElmer Informatic, Inc.	https://revvitysignals.com/products/research/chemdraw
Maestro, Version 13.0	Schrödinger	https://www.schrodinger.com

Mnova	Mestrelab Research	https://mestrelab.com
Prism 10	GraphPad Software	https://www.graphpad.com/
PyMOL 2.5	Schrödinger	https://pymol.org/2/

Characterization of compounds

NMR spectra were recorded on AVIIIHD 500 or 600 MHz Bruker spectrometers. The spectra were calibrated to the residual ^{1}H and ^{13}C signals of the solvents. Chemical shifts are reported in ppm. Multiplicities are abbreviated as follows: singlet (s), doublet (d), doublet-doublet (dd), multiplet (m). High resolution electrospray ionization mass spectrometry, HRMS (ESI), were obtained on a Thermo Exactive Plus Orbitrap or a Bruker Maxis Impact QTOF. The purity of compound **2** was assessed via NMR as the high polarity and lack of chromophore of the compound rendered it unsuitable for an LC-MS purity assessment. The concentration of **IP6** and compound **2** used in the *in vitro* experiments was determined via ^{1}H NMR using an internal standard. Compound **2** was lyophilized (Christ Alpha 2–4 LDplus) prior to usage to ensure dryness.

Synthetic methods

All reagents were used as received unless otherwise noted. Solvents were purchased in the best quality available, anhydrous solvents were stored under nitrogen and dried over activated molecular sieves (4 Å, 1.6–2.6mm, Sigma-Aldrich). Reactions were monitored by thin layer chromatography (TLC) using SiliCycle TLC silica gel 60 F254 with UV light (254 nm) as a visualizing agent and acidic ceric ammonium molybdate (CAM) as the developing agent. Purification was achieved by either: flash column chromatography with silica gel (230–400 mesh), a size-exclusion column with sephadex LH-20, or ion-exchange chromatography with a sodium charged Dowex 50WX8, 50–100 mesh resin. The Dowex resin was purchased in its protonated form and was converted to the sodium charged form by washing the resin with milli-Q H_2O until a neutral pH was achieved, charging with 1 M NaOH until a basic pH was achieved, and washing again with milli-Q H_2O until a neutral pH was achieved. No unexpected or unusually high safety hazards were encountered during this work.

3. Experimental Procedures and Synthesis

(1) Experimental Procedures

Phytase Degradation Assay

In a 1.5 mL microcentrifuge tube, 4 mM of **IP6** or **IT6** were dissolved in 100 mM acetate buffer, pH 5, 10% D_2O with 4 mM TMP as an internal standard. Immediately prior to placing the sample in an NMR tube, 0.482 mg/mL of phytase-4 (Creative Enzymes) was added to achieve a final volume of 600 µL. The ^{31}P NMR were acquired on a Bruker AVIIIHD 500 MHz NMR Spectrometer with a HX (X = ^{109}Ag-^{19}F) probe. ^{31}P NMR spectra had ^{1}H-decoupling and were collected at 300 K with 256 scans. ^{31}P NMR were collected at the time points: 0, 1, 2, 4, 8, 16, 24, and 32 h. The concentration of **IP6** or **IT6** was determined for each time point in respect to the peak integration of the internal standard. Each concentration was then made relative to the concentration determined at time 0 h, to give the percentage of starting material in the NMR tube. The percent of **IT6** or **IP6** was plotted against time (h) in Prism 10, n = 3, mean ± SD.

Calculated LogP (cLogP) Determination

The structure of compounds **IP6-Bn** and **IT6-Bn** were drawn in ChemDraw and the cLogP was calculated through the built-in BioByte plugin.

Hückel Calculation

The SMILES for **IT6-Bn** and **IP6-Bn** were imported into Chem3D (PerkinElmer) and geometry optimization/energy minimization was performed, the minimum root mean square (RMS) gradient was set to 0.100. Next, the extended Hückel molecular orbital (HMO) charge calculations were performed in Chem3D. This software was also used to display the distribution of the calculated Hückel charge on the energy minima structure by coloring the atoms in correspondence with its partial charge. The difference between the partial charge for each molecular mechanics (MM2) atom type on **IT6-Bn** and **IP6-Bn** was compared to zero via a Welch's t-test in Prism 10, p-values were listed for each set of comparisons. In addition, the polar surface area of **IP6-Bn** and **IT6-Bn** was calculated in Chem3D on the energy minimized structures.

Polarity Chromatogram

40 mg/mL of **IP6-Bn** or **IT6-Bn** in dichloromethane (DCM) were added to a 4 g 40–63 µm 60 Å SepaFlash column (Santai Technologies, Inc., S-5101-0004). The column was attached to a CombiFlash Rf+ automated UV flash chromatography (Teledyne Isco) system. The solvent was

run at a flow rate of 18 mL/min, with 0–10% methanol/DCM over 16 minutes. The correspondent chromatogram was taken at a wavelength of 215 nm.

Precipitation Assay

In a 1.5 mL microcentrifuge tube, 4 mM of **IP6** or **IT6** were dissolved in 100 mM tris buffer, pH 7.4, and varied concentrations of $CaCl_2$ were added to achieve the final concentrations: 0, 1, 2, 4, 8, 16, 32, 64, and 128 mM $CaCl_2$ with a final volume of 540 µL. Each sample was vortexed for 30 s and then left at room temperature for 30 min. The samples were centrifuged for 5 min at 3500 xg (Eppendorf Centrifuge 5425 R). The supernatant was isolated and 60 µL of TMP in 100 mM tris, pH 7.4 in D_2O was added as an internal standard with a final concentration of 4 mM. The samples were pipetted into 8-inch 5 mm O.D NMR tubes (Fisher Scientific). The ^{31}P NMR were acquired on a Bruker AVIIIHD 500 MHz NMR Spectrometer with a HX (X = ^{109}Ag-^{19}F) probe. ^{31}P NMR spectra had ^{1}H coupling and were collected at 300 K with 128 scans. The concentration of **IP6** or **IT6** was determined for each $CaCl_2$ concentration based off of the peak integration in comparison with that of TMP. The concentration of **IT6** or **IP6** was plotted against the $CaCl_2$ concentration in Prism 10. The plot was curve fit with a plateau followed by one phase decay nonlinear curve fit. The best-fit value for the primary inflection point that corresponds with the x-axis (X_0) was used to determine the concentration of $CaCl_2$ required to precipitate **IP6** or **IT6** from a pH 7.4 solution. The ratio (n) of base [B^-] versus acid [A^+] was determined with this value.

Differential Light Scattering (DLS)

In a 1.5 mL microcentrifuge tube, 4 mM of **IP6** or **IT6** were dissolved in 100 mM tris buffer, pH 7.4, and varied concentrations of $CaCl_2$ were added to achieve the final concentrations: 0, 1, 2, 4, 8, 16, 32, and 64 mM $CaCl_2$ with a final volume of 600 µL. Each sample was vortexed for 30 s and then left at room temperature for 30 min. The solutions were analyzed by DLS on a Malvern Panalytical Zetasizer Nano ZS. The hydrodynamic diameters of **IP6** and **IT6** were measured using a Zetasizer Nano ZS90 DLS system equipped with a red (633 nm) laser and an Avalanche photodiode detector (APD) (quantum efficiency > 50% at 633 nm) (Malvern Instruments Ltd., England). A Hellma cuvette QS 3 mm was used as a sample container. DTS applications 5.10 software was used to analyze the data. All sizes reported here were based on intensity average. The intensity average particle size was obtained using a non-negative least squares (NNLS) analysis

method. For each sample, four DLS measurements were conducted with a fixed 10 runs and each run lasts 10 s. A detection angle of 90° was chosen for the size measurement.

Table S3. Mean diameter by intensity and polydispersity index (PDI) of **IP6** or **IT6** aggregates based on DLS analysis.

$CaCl_2$ Concentration (mM)	**IP6**		**IT6**	
	Mean Diameter (nm)	PDI	Mean Diameter (nm)	PDI
0	34.60 ± 6.31	0.570 ± 0.123	618.57 ± 43.14	0.082 ± 0.042
1	-	-	576.64 ± 268.97	0.216 ± 0.022
2	-	-	312.23 ± 18.88	0.046 ± 0.048
4	259.87 ± 53.43	0.198 ± 0.013	632.27 ± 119.71	0.154 ± 0.041
8	574.93 ± 85.57	0.282 ± 0.014	781.50 ± 13.90	0.220 ± 0.011
16	3,107.98 ± 627.75	0.367 ± 0.032	776.62 ± 208.94	0.204 ± 0.045
32	8,398.59 ± 377.06	0.432 ± 0.104	7,697.83 ± 1,276.87	0.315 ± 0.089
64	-	-	9,968.97 ± 14.89	0.206 ± 0.119
128	-	-	9,276.11 ± 1,207.19	0.251 ± 0.098

Expression and Purification of AvrA and VopA

The expression of AvrA was performed as described previously.[1] The expression construct for AvrA and VopA were synthesized by Integrated DNA Technologies (Coralville, IA) with restriction sites for cloning into a modified pET28b vector containing a Ulp cleavable, N- terminal His-SUMO tag.[2] AvrA and VopA plasmids were transformed into *Escherichia coli* BL21(DE3) pLysS by standard techniques. Overnight cultures of transformed BL21(DE3) were diluted 100-fold into lysogeny broth (LB) containing 50 μg/mL kanamycin and grown at 37°C until an OD_{600} of 0.7−0.9 was reached. 1 mM isopropyl β-D-1-thiogalactopyranoside (IPTG) was added and the cultures were grown at 20°C for 16−20 h. The cultures were pelleted by centrifugation at 5,000 xg (Eppendorf Centrifuge 5425 R) for 15 min. Pellets were suspended in NiA buffer (500 mM NaCl, 10% glycerol, 10 mM imidazole, and 20 mM tris, pH 8.0 at 4°C) supplemented with DNase and 100 μM phenylmethanesulfonyl fluoride and lysed in a probe sonicator (Emulsifex C3). The crude lysate was cleared by ultracentrifugation at 50,000 xg (Beckman coulter 44798) for 1 h, and the supernatant was collected. AvrA or VopA was applied to a column containing Ni^+ affinity resin (Thermo Scientific). The samples were washed with 5 column volumes of NiA containing 3% NiB buffer (NiA with 1 M imidazole) and eluted with 30% NiB. Relevant fractions were pooled, and

ubiquitin-like protein (Ulp) was added at a ratio of 1:1000 (w/w). AvrA or VopA was dialyzed overnight into NiA buffer, followed by reapplication to Ni^{+} resin to remove the free His-SUMO tag and uncleaved protein. The sample was then applied to a 4.7 mL Mono-Q column (GE Healthcare) in 20 mM tris, pH 8 and eluted with a 0–50% gradient of 1 M NaCl. Finally, AvrA or VopA was applied to a Superdex 200 increase analytical column (GE Healthcare) and equilibrated with 20 mM tris, 100 mM NaCl, pH 7.4, 1 mM DTT.

Expression and Purification of TcdB CPD

The expression of the TcdB CPD was performed as described previously.[3] To generate the truncated cysteine protease domain (tCPD) from TcdB (TcdB 543-799 His6), the nucleotide sequence coding for amino acids 543—799 of TcdB was used. The pET22b-$TcdB_{543\text{-}799}$ plasmid was kindly donated by Dr. Matthew Bogyo and Dr. Aimee Shen, Stanford University. The plasmid was transformed into *Escherichia coli* BL21(DE3) by standard techniques. Overnight cultures of transformed BL21(DE3) were diluted 1:100 in 2 L Terrific Broth and grown at 37ºC until an OD_{600} of 0.8—0.9 was reached. IPTG was added and the cultures were grown for 3.5 h at 30ºC. The cultures were pelleted by centrifugation at 5,000 x *g* for 30 min at 4ºC (Beckman J2-21, JS5.3). The cell pellets were resuspended in sonication buffer (20 mM phosphate, 100 mM NaCl, 1 mM $MgCl_2$, pH 8). The cell lysates were shaken for 30 min at 4ºC and then sonicated with a probe sonicator (Misonix Sonicator 3000). The cells were centrifuged at 5,000 x *g* for 30 min at 4ºC, then the supernatant was collected. TcdB CPD was purified from the cleared lysate by metal-ion affinity chromatography using Co-NTA resin (ThermoFisher Scientific) at 4ºC. Eluted fractions containing protein were placed on a size exclusion gel filtration column (Superdex 75 HiLoad Prep column) at 4ºC and eluted into the desired buffer.

Isothermal Calorimetry (ITC)

ITC measurements were performed on the MicroCal iTC200 (Malvern Panalytical). All AvrA samples were prepared in a 20 mM HEPES, 200 mM NaCl, 5% glycerol, 1 mM TCEP, pH 7.4 buffer. The sample cell contained 280 µL of 53 µM AvrA in the same HEPES buffer. AvrA was prepared the day of the ITC experiment due to protein instability. A total of 39 µL of 530 µM **IP6** or **IT6** in HEPES buffer was titrated into the sample cell with 29 successive injections at 20ºC. All TcdB CPD samples were prepared in a 20 mM Tris, 150 mM NaCl, 1 mM TCEP, pH 7.4 buffer.

For the TcdB CPD samples the sample cell contained 280 μL of 53 μM TcdB CPD in the same Tris buffer. TcdB CPD was prepared the day of the ITC experiment due to protein instability. A total of 39 μL of 530 μM **IP6** or **IT6** in Tris buffer was titrated into the sample cell with 29 successive injections at 20ºC. The buffers for TcdB CPD and AvrA were selected by screening the proteins in different buffering conditions via differential scanning fluorometry to determine the buffering conditions corresponding with the highest melting temperature (T_M). All samples were degassed and thermostated prior to measurements. Heat of dilution (HOD) runs were measured by injecting 530 μM **IP6** or **IT6** into HEPES buffer alone. HOD measurements were subtracted from the corresponding thermal peaks measured for the sample prior to data analysis. The resulting differential binding heat spectra were prepared for publication in the MicroCal ORIGIN software using the one site model fitting. The differential binding heat data were analyzed with the AFFINImeter software using the one site model fitting. Errors were derived from fitting statistics. The differential binding heat data was also used to determine the k_{off} values from the equilibration time curve by the kinITC methodology using the AFFINImeter software.[4,5]

Differential Scanning Fluorometry

Differential scanning fluorometry (DSF) was performed with AvrA and VopA at a final concentration of 0.4 μg/mL in 20 mM HEPES, 200 mM NaCl, 5% glycerol, 1 mM TCEP, pH 7.4. AvrA or VopA were combined with 4X SYPRO Orange, and a serial dilution of **IP6** or **IT6**. Protein used for this experiment was prepared the same day due to protein instability. A CFX Connect Real-Time System qRT-PCR thermocycler (Bio-Rad) was used to establish a temperature gradient from 25ºC to 95ºC in 0.2ºC increments, while simultaneously recording the increase in SYPRO Orange fluorescence over 10 sec. The Bio-Rad CFX Connect Manager software was used to integrate the fluorescence curves to calculate the melting temperature (T_M). The T_M for AvrA or VopA with ligand was subtracted from the T_M of protein alone to calculate ΔT_M. The ΔT_M for AvrA or VopA with **IP6** or **IT6** was then plotted against the logarithm of the concentration of each IP6 analog. The resultant plot was fit with a nonlinear curve fit in Prism 10 (Variable slope, 4 parameters), the A2 values were used to determine the maximum change in ΔT_M induced by the presence of **IP6** or **IT6**.

Docking with AvrA and **IT6**

Docking experiments were performed using the Glide program within the Maestro software (Version 13.0; Schrödinger).[6,7] The AvrA protein structure (PDB: 6BE0) was obtained from the Protein Data Bank and prepared within the Protein Preparation Wizard.[1] Missing side chains and hydrogens were added, the structure was relaxed with the OPLS4 force field and water molecules were removed.[8] A receptor grid centered at the **IP6** binding site was generated with the Glide tool.[6] The fully deprotonated **IT6** structure was prepared using the 2D Sketcher tool.[3] The top docking pose was obtained using the Glide XP extra precision module with flexible ligand sampling.[7] Poses were minimized after docking. The protocol was verified against the cognate molecule, **IP6**.

(2) Synthesis

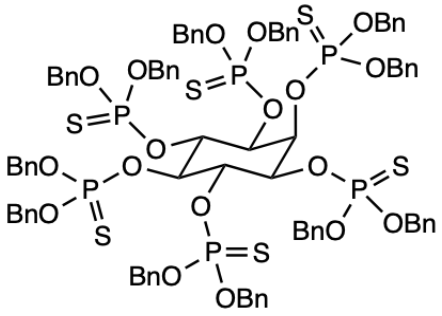

***Myo*-inositol hexakis-dibenzylthiophosphate (1)**

Synthesis of **1** was performed as described previously.[9] To a stirred suspension of *myo*-inositol (97 mg, 0.54 mmol) in an anhydrous mixture of DMF (14 mL) and CH_3CN (4 mL) 1*H*-tetrazole (14 mL, 0.45 M in CH_3CN) and dibenzyl-*N*,*N*-diisopropyl phosphoramidite (1.34 mL, 3.98 mmol) were added under a nitrogen atmosphere. The mixture was stirred at room temperature for 24 h. Thereafter, pyridine (0.40 mL) and carbon disulfide (0.40 mL, 6.84 mmol) were added, followed by sulfur (427 mg, 13.34 mmol). The reaction was stirred at room temperature overnight then diluted with ethyl acetate (150 mL), washed with $NaHCO_3$ saturated solution (100 mL), brine (100 mL), dried ($MgSO_4$), filtered, and concentrated *in vacuo*. Purification was achieved by flash chromatography on silica gel (5, 10, 15, and 20% ethyl acetate/cyclohexane) to afford compound **1** as a clear oil (236 mg, 0.13 mmol, 24% yield).

SMILES S=P(OCC1=CC=CC=C1)(OCC2=CC=CC=C2)O[C@@H]3[C@H](OP(OCC4=CC=CC=C4)(OCC5=CC=CC=C5)=S)[C@@H](OP(OCC6=CC=CC=C6)(OCC7=CC=CC=C7)=S)[C@H](OP(OCC8=CC=CC=C8)(OCC9=CC=CC=C9)=S)[C@@H](OP(OCC%10=CC=CC=C%1

0)(OCC%11=CC=CC=C%11)=S)[C@@H]3OP(OCC%12=CC=CC=C%12)(OCC%13=CC=CC=C%13)=S

^{1}H NMR (600 MHz, $CDCl_3$): δ 7.39–7.06 (m, 60H, H_{Ph}), 5.61–5.55 (m, 3H, H_2, H_4, H_6), 5.49–5.46 (m, 2H, H_1–H_3), 5.34 (d, J = 15.8 Hz, 1H, H_5), 5.19–5.00 (m, 24H, CH_2).

^{1}H NMR spectrum is in agreement with the literature report.[9]

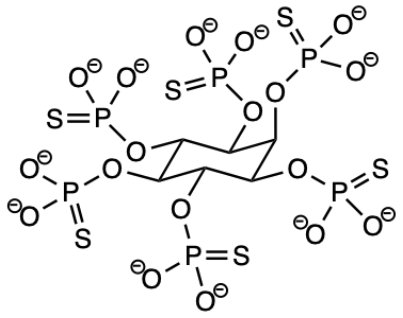

Hexakis-thiophosphate (2)

Synthesis of **2** was performed as described previously.[9] To a stirred solution of compound **1** (235 mg, 0.13 mmol) in anhydrous THF (4 mL) liquid NH_3 (20 mL) was added at -78°C under a nitrogen atmosphere. Sodium was added in small pieces until the solution turned dark blue. The reaction was stirred for 10 min then quenched with a saturated NH_4Cl solution. NH_3 was slowly evaporated overnight, and the remaining solution was extracted with CH_2Cl_2 (10 mL). Purification of the aqueous layer was achieved by Sephadex LH-20 (100% H_2O), the compound was then charged with sodium counterions via a sodium charged Dowex 50WX8 column (100% H_2O). Finally, freeze-drying afforded the sodium form of compound **2** as a white lyophilizate (57 mg, 59 µmol, 47% yield). Compound **2** had 98% purity by ^{1}H NMR.

SMILES [O-]/S([O-])=P\O[C@@H]1[C@H](O/P=S([O-])\[O-])[C@@H](O/P=S([O-])\[O-])[C@H](O/P=S([O-])\[O-])[C@@H](O/P=S([O-])\[O-])[C@@H]1O/P=S([O-])\[O-]

^{1}H NMR (600 MHz, D_2O): δ 4.87 (d, J = 13.4 Hz, 2H, H_4–H_6), 4.83 (d, J = 11.8 Hz, 2H, H_1–H_3), 4.72 (d, J = 14.5 Hz, 1H, H_2), 4.55 (d, J = 14.1 Hz, 1H, H_5).

^{1}H NMR spectrum is in agreement with the literature report.[9]

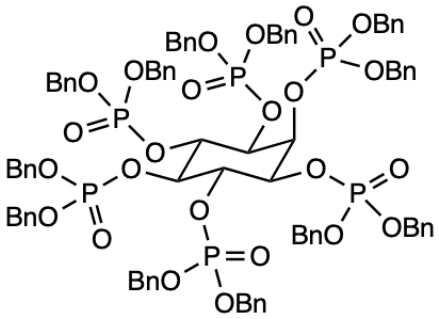

***Myo*-inositol hexakis-dibenzylphosphate (3)**

To a stirred solution of *myo*-inositol (0.1045 g, 0.58 mmol) in a mixture of anhydrous DCM (9.67 mL), 5-phenyl-1*H*-tetrazole (0.8477 g, 5.8 mmol), and dibenzyl-*N*,*N*-diisopropyl phosphoramidite (1.516 mL, 4.06 mmol) were added under N_2 atmosphere. The reaction mixture was stirred at room temperature for 24 h. The reaction was then cooled to -20°C and 3-chloroperbenzoic acid (1.300 g, 5.8 mmol) was added portionwise while stirring for 15 min. The cooling bath was removed, and the reaction was allowed to reach room temperature. The solution was then diluted with DCM (50 mL), washed with 10% sodium sulfite solution (50 mL) thrice, dried ($MgSO_4$), filtered, and concentrated *in vacuo*. Purification was achieved over two steps. First, by flash chromatography on silica gel (40, 50, 60% ethyl acetate/cyclohexane) and second by reverse phase chromatography (65, 75, 85% acetonitrile/H_2O) to afford compound **3** as a clear oil (0.178 g, 0.1023 mmol, 18% yield).

SMILES O=P(OCC1=CC=CC=C1)(OCC2=CC=CC=C2)O[C@@H]3[C@H](OP(OCC4=CC=CC=C4)(OCC5=CC=CC=C5)=O)[C@@H](OP(OCC6=CC=CC=C6)(OCC7=CC=CC=C7)=O)[C@H](OP(OCC8=CC=CC=C8)(OCC9=CC=CC=C9)=O)[C@@H](OP(OCC%10=CC=CC=C%10)(OCC%11=CC=CC=C%11)=O)[C@@H]3OP(OCC%12=CC=CC=C%12)(OCC%13=CC=CC=C%13)=O

^{1}H NMR (600 MHz, D_2O): δ 7.34–7.30 (m, 4H, H_{Ph}), 7.27–7.11 (m, 56H, H_{Ph}), 5.64 (d, J = 8.86 Hz, 1H, H_2), 5.27–5.21 (dd, J = 11.75, 6.06 Hz, 2H, H_{CH2}), 5.17–5.11 (dd, J = 11.75, 7.02 Hz, 2H, H_{CH2}), 5.11–5.02 (m, 16H, H_{CH2}, H_4, H_6), 5.02–4.93 (m, 6H, H_{CH2}).

^{31}P NMR (203 MHz, D_2O): δ -0.87 (2P), -0.96 (1P), -1.56 (2P), -2.55 (1P).

^{13}C NMR (151 MHz, D_2O): δ 135.98 (C_{Ph}), 135.96 (C_{Ph}), 135.93 (C_{Ph}), 135.92 (C_{Ph}), 135.89 (C_{Ph}), 135.80 (C_{Ph}), 135.74 (C_{Ph}), 135.72 (C_{Ph}), 135.70 (C_{Ph}), 135.67 (C_{Ph}), 135.65 (C_{Ph}), 128.51 (C_{Ph}), 128.44 (C_{Ph}), 128.43 (C_{Ph}), 128.36 (C_{Ph}), 128.35 (C_{Ph}), 128.31 (C_{Ph}), 128.23 (C_{Ph}), 128.20 (C_{Ph}),

128.15 (C_{Ph}), 128.01 (C_{Ph}), 127.90 (C_{Ph}), 74.58 (C_2), 73.42 (C_5), 70.10 (C_4, C_6), 70.07 (C_1, C_3), 69.88 (CH_2), 69.85 (CH_2), 69.84 (CH_2), 69.80 (CH_2), 69.76 (CH_2), 69.75 (CH_2), 69.71 (CH_2), 69.67 (CH_2).

HRMS FTMS E$^+$. Calcd for $C_{90}H_{90}O_{24}NaP_6$ $[M+Na]^+$ 1763.41; found: 1763.4140.

4. NMR Spectra

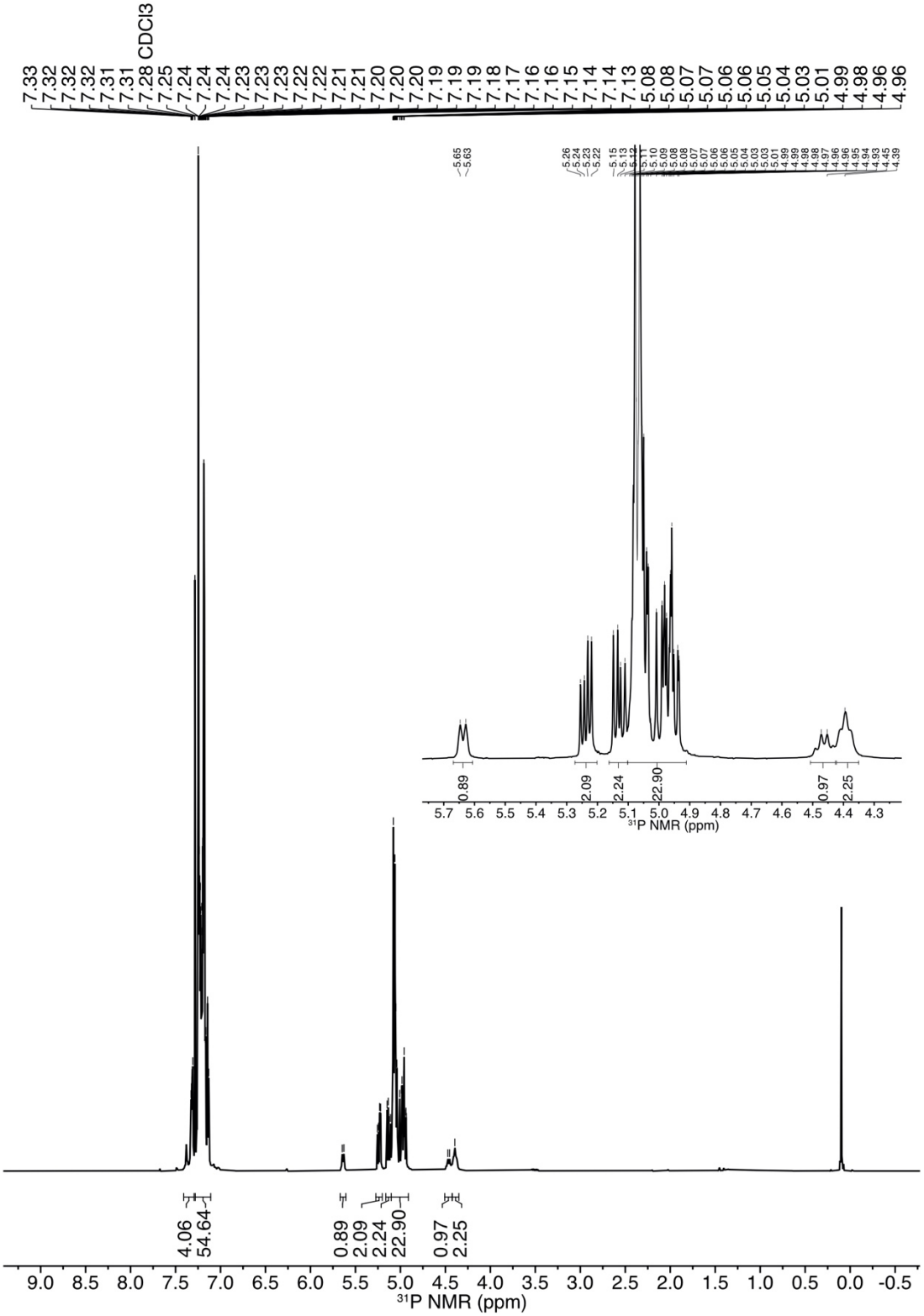

Figure S9. ^{1}H NMR of hexakis-dibenzylphosphate.

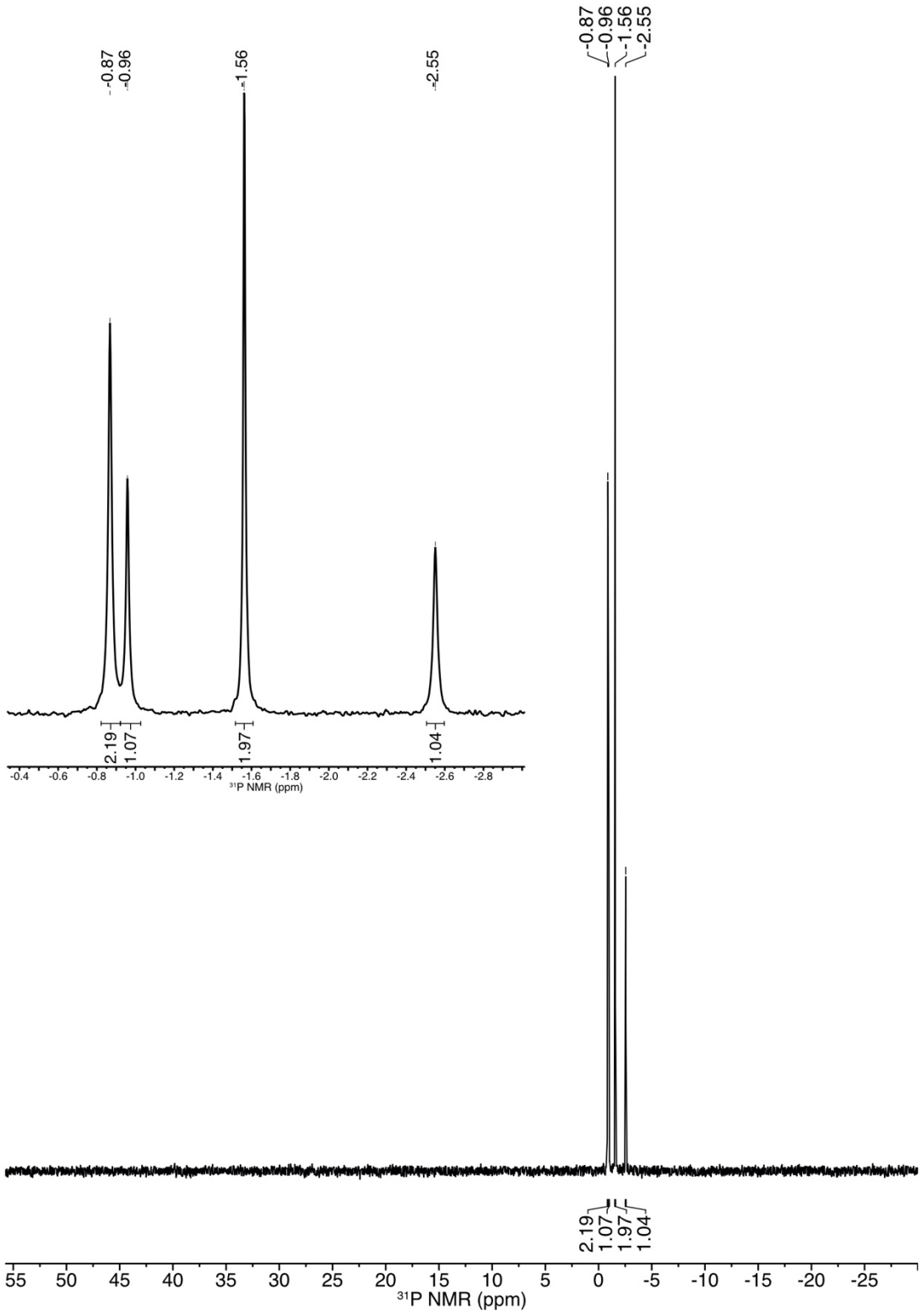

Figure S10. ^{31}P NMR of hexakis-dibenzylphosphate.

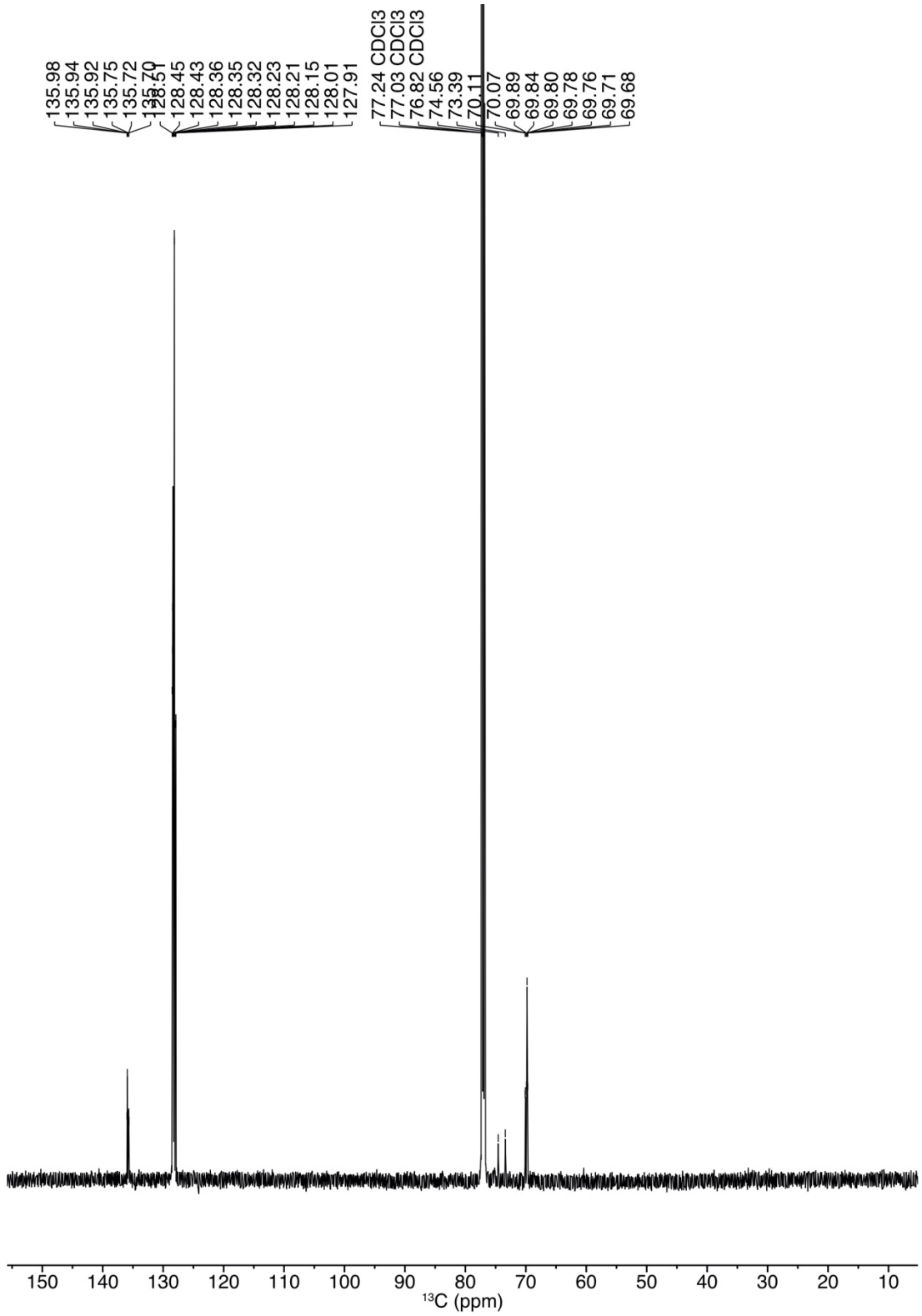

Figure S11. ^{13}C NMR of hexakis-dibenzylphosphate.

5. References

1 J. M. Labriola, Y. Zhou and B. Nagar, *Biochemistry*, 2018, **57**, 4985–4996.

2 E. Mossessova and C. D. Lima, *Mol. Cell*, 2000, **5**, 865–876.

3 R. Cummer, F. Grosjean, R. Bolteau, S. E. Vasegh, S. Veyron, L. Keogh, J.-F. Trempe and B. Castagner, 2024, preprint, DOI: 10.26434/chemrxiv-2024-2cf6g-v2.

4 D. Burnouf, E. Ennifar, S. Guedich, B. Puffer, G. Hoffmann, G. Bec, F. Disdier, M. Baltzinger and P. Dumas, *J. Am. Chem. Soc.*, 2012, **134**, 559–565.

5 Á. Piñeiro, E. Muñoz, J. Sabín, M. Costas, M. Bastos, A. Velázquez-Campoy, P. F. Garrido, P. Dumas, E. Ennifar, L. García-Río, J. Rial, D. Pérez, P. Fraga, A. Rodríguez and C. Cotelo, *Anal. Biochem.*, 2019, **577**, 117–134.

6 R. A. Friesner, J. L. Banks, R. B. Murphy, T. A. Halgren, J. J. Klicic, D. T. Mainz, M. P. Repasky, E. H. Knoll, M. Shelley, J. K. Perry, D. E. Shaw, P. Francis and P. S. Shenkin, *J. Med. Chem.*, 2004, **47**, 1739–1749.

7 R. A. Friesner, R. B. Murphy, M. P. Repasky, L. L. Frye, J. R. Greenwood, T. A. Halgren, P. C. Sanschagrin and D. T. Mainz, *J. Med. Chem.*, 2006, **49**, 6177–6196.

8 C. Lu, C. Wu, D. Ghoreishi, W. Chen, L. Wang, W. Damm, G. A. Ross, M. K. Dahlgren, E. Russell, C. D. Von Bargen, R. Abel, R. A. Friesner and E. D. Harder, *J. Chem. Theory Comput.*, 2021, **17**, 4291–4300.

9 D. Chen, N. Oezguen, P. Urvil, C. Ferguson, S. M. Dann and T. C. Savidge, *Sci. Adv.*, 2016, **2**, e1501240.